

MULTI-OBJECTIVE OPTIMIZATION OF ORGANIC RANKINE CYCLE POWER PLANTS USING PURE AND MIXED WORKING FLUIDS

Jesper G. Andreasen ^{1*}, Martin R. Kærn¹, Leonardo Pierobon ¹, Ulrik Larsen ², Fredrik Haglind ¹

¹ Technical University of Denmark, Building 403, Nils Koppels Allé, DK-2800 Kgs. Lyngby, Denmark. jgan@mek.dtu.dk*, pmak@mek.dtu.dk, lpier@mek.dtu.dk, frh@mek.dtu.dk

² Department of Shipping and Marine Technology, Chalmers University of Technology, SE-412 96 Gothenburg, Sweden. ulrik.larsen@chalmers.se

* Corresponding Author

ABSTRACT

For zeotropic mixtures, the temperature varies during phase change, which is opposed to the isothermal phase change of pure fluids. The use of such mixtures as working fluids in organic Rankine cycle power plants enables a minimization of the mean temperature difference of the heat exchangers when the minimum pinch point temperature difference is kept fixed. A low mean temperature difference means low heat transfer irreversibilities, which is beneficial for cycle performance, but it also results in larger heat transfer surface areas. Moreover, the two-phase heat transfer coefficients for zeotropic mixtures are usually degraded compared to an ideal mixture heat transfer coefficient linearly interpolated between the pure fluid values. This entails a need for larger and more expensive heat exchangers. Previous studies primarily focus on the thermodynamic benefits of zeotropic mixtures by employing first and second law analyses. In order to assess the feasibility of using zeotropic mixtures, it is, however, important to consider the additional costs of the heat exchangers. In this study, we aim at evaluating the economic feasibility of zeotropic mixtures compared to pure fluids. We carry out a multi-objective optimization of the net power output and the component costs for organic Rankine cycle power plants using low-temperature heat at 90 °C to produce electrical power at around 500 kW. The primary outcomes of the study are Pareto fronts, illustrating the power/cost relations for R32, R134a and R32/R134a (0.65/0.35_{mole}). The results indicate that R32/134a is the best of these fluids, with 3.4 % higher net power than R32 at the same total cost of 1200 k\$.

1. INTRODUCTION

The organic Rankine cycle (ORC) power plant is a technology that enables the utilization of low-temperature heat for electricity production. The working fluid selection for the ORC power plant is a critical design decision which affects the thermodynamic performance and the economic feasibility of the plant. The use of zeotropic mixtures as working fluids has been proposed as a way to improve the performance of the cycle (Angelino and Colonna, 1998). Zeotropic mixtures change phase with varying temperature, which is opposed to the isothermal phase change of pure fluids. As the temperature of the heat source and heat sink change during heat exchange, zeotropic working fluids enable a closer match of the temperature profiles in the condenser and the boiler, compared to pure fluids. This results in a decrease in heat transfer irreversibilities and an increase in cycle performance. The condenser has been identified as the component where the irreversibilities decrease the most when using mixed working fluids (Heberle et al., 2012; Lecompte et al., 2014), and the increment in cycle performance when using zeotropic mixtures instead of pure fluids is largest when the heat source temperature is low (Chys et al., 2012).

Heberle et al. (2012) optimized the performance of ORC systems using zeotropic working fluids for utilization of geothermal heat at 120 °C. Compared to pure isobutane, a mixture of isobutane/isopentane (0.9/0.1_{mole}) achieved an increase in the second law efficiency of 8 %. They also compared the UA -values (the product of the overall heat transfer coefficient and the heat transfer area) of the heat exchangers in the cycle, and found that the mixture compositions resulting in the highest cycle performance also required the highest UA -values. This suggests that the cost of heat exchangers is larger when the mixture is used. Le et al. (2014) performed maximizations of the exergy efficiency and minimizations of the levelized cost of electricity for ORC systems using mixtures of R245fa and pentane as working fluids. Pure pentane was identified as the best fluid, in both optimizations. In the minimization of the levelized cost of electricity, the minimum value for pentane was found to be 0.0863 \$/kWh. The mixtures pentane/R245fa (0.05/0.95_{mass}) and pentane/R245fa (0.1/0.9_{mass}) obtained similar values at 0.0872 and 0.0873 \$/kWh, respectively.

In the present study, we carry out a multi-objective optimization of net power output and component cost for an ORC power plant utilizing a low-temperature water stream at 90 °C. The objective of the study is to investigate and compare the relationship between cost and performance for ORC power plants using pure fluids and zeotropic mixtures as working fluids. The fluids considered are R32, R134a and R32/R134a (0.65/0.35_{mole}). These fluids are selected, since they achieved high thermodynamic performance at subcritical turbine inlet pressure in a previous study (Andreasen et al., 2014).

Previous studies (e.g. (Heberle et al., 2012; Trapp and Colonna, 2013; Andreasen et al., 2014)) which compare pure fluids and zeotropic mixtures focus mainly on the evaluation of the thermodynamic performance of the fluids. These studies indicated that the thermodynamic performance can be increased by using zeotropic mixtures as working fluids, while the size and thereby the cost of the heat exchangers increase. In order to evaluate the feasibility of zeotropic mixtures, it is, therefore, necessary also to assess the cost of equipment such that the working fluids are compared based on the same investment costs. Le et al. (2014) included a single-objective optimization of the levelized cost of electricity. However, they did not consider the simultaneous optimization of thermodynamic performance and cost as is done in the present study. It is advantageous to implement the multi-objective optimization since it enables a comparison of fluid performance based on the same equipment costs.

The paper begins with a description of the methodology in Section 2. The results are presented and discussed in Section 3 and conclusions are given in Section 4.

2. METHODS

The multi-objective optimization method is developed in Matlab version 2014b (Mathworks, 2014) based on the framework described by Pierobon et al. (2014). The steady state ORC system model, capable of handling both pure fluids and mixtures through REFPROP[®] version 9.1 (Lemmon et al., 2013), is adapted from a previous study (Andreasen et al., 2014) and integrated within the simulation tool. A sketch of the ORC power plant is depicted in Figure 1.

The heat source is a low-temperature water stream as investigated in Andreasen et al. (2014). Table 1 shows the hot fluid parameters along with the fixed input parameters assumed for the cycle. The hot fluid and cooling water pumps are denoted as auxiliary pumps.

The optimization variables include cycle and heat exchanger design parameters; see Table 2. The lower boundary for the turbine inlet pressure is defined as the bubble point pressure at a temperature 30 °C higher than the cooling water inlet temperature ($T_{cool,i}$), and the upper boundary is 90 % of the critical pressure (P_c). The superheating degree is defined as the temperature difference between the dew point temperature and the turbine inlet temperature, and the bounds for the baffle spacing are set relative to the shell diameter (d_s). The lower bounds for the pinch points in the condenser and the boiler are set to 0.1 °C. Such low pinch points are not feasible in practice, but they are allowed in this study in order to

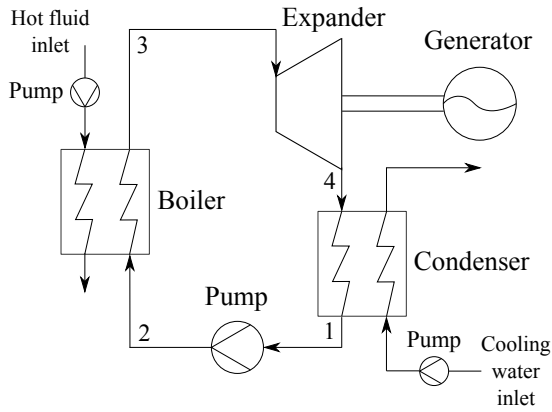


Figure 1: Organic Rankine cycle power system

Table 1: ORC system modelling conditions

| Parameter description | Value | Unit |
|---------------------------------|-------|------|
| <i>Hot fluid (water)</i> | | |
| Hot fluid inlet temperature | 90 | °C |
| Hot fluid mass flow | 50 | kg/s |
| Hot fluid pressure | 4 | bar |
| <i>Condenser</i> | | |
| Cooling water inlet temperature | 15 | °C |
| Outlet vapour quality | 0 | - |
| Cooling water pressure | 4 | bar |
| <i>Working fluid pump</i> | | |
| Isentropic efficiency | 0.8 | - |
| <i>Auxiliary pumps</i> | | |
| Isentropic efficiency | 0.7 | - |
| <i>Turbine</i> | | |
| Isentropic efficiency | 0.8 | - |
| Minimum outlet vapour quality | 1 | - |

compare the fluids based on a wide range of equipment costs.

The objective functions for the optimization are the net power output and the total cost of the components. The net power is calculated as

$$\dot{W}_{NET} = \dot{m}_{wf}(h_3 - h_4 - (h_2 - h_1)) - \dot{W}_{aux.,pumps} \quad (1)$$

where \dot{m}_{wf} is the working fluid mass flow, h is the mass specific enthalpy and $\dot{W}_{aux.,pumps}$ is the power consumption of the hot fluid and cooling water pumps. The total cost (C_{tot}) of the components is found by adding the cost of the turbine (C_{turb}), working fluid pump ($C_{wf,pump}$), condenser (C_{cond}), boiler (C_{boil}), generator (C_{gen}) and the two auxiliary pumps ($C_{aux.,pumps}$)

$$C_{tot} = C_{turb} + C_{wf,pump} + C_{cond} + C_{boil} + C_{gen} + C_{aux.,pumps} \quad (2)$$

The total cost considered in this paper is the equipment cost, thus further expenses are expected for the construction of the ORC power plants, e.g. installation costs.

Table 2: Optimization variables

| Parameter description | Lower bound | Upper bound | Unit |
|-----------------------------------|----------------------------|-------------------|------|
| <i>Cycle parameters</i> | | | |
| Turbine inlet pressure | $P_{bub}(T_{cool,i} + 30)$ | $0.9 \cdot P_c$ | bar |
| Superheating degree | 0 | 40 | °C |
| Condensing temperature | $T_{cool,i} + 5$ | $T_{cool,i} + 20$ | °C |
| Boiler pinch point temperature | 0.1 | 20 | °C |
| Condenser pinch point temperature | 0.1 | 20 | °C |
| <i>Condenser design</i> | | | |
| Inner tube diameter | 16 | 26 | mm |
| Number of tubes | 10 | 200 | - |
| Baffle spacing | $0.5 \cdot d_s$ | $3 \cdot d_s$ | mm |
| <i>Boiler design</i> | | | |
| Inner tube diameter | 16 | 26 | mm |
| Number of tubes | 10 | 200 | - |
| Baffle spacing | $0.5 \cdot d_s$ | $3 \cdot d_s$ | mm |

The optimization framework comprises the following steps (Pierobon et al., 2014):

- Calculation of the process states by use of the cycle model (without pressure losses)
- Layout of the geometry of the condenser and the boiler and calculation of the heat transfer area and the pressure losses
- Calculation of the net power output by use of the cycle model (with pressure losses)

- Calculation of the total component cost

2.1 Heat Exchanger Modelling

The heat exchanger models are developed based on the shell-and-tube model used in Kærn et al. (2015). In order to avoid leakage of working fluid, which for zeotropic mixtures can result in undesirable composition shifts, both the boiler and the condenser are designed with the working fluid flowing inside the tubes (Cavallini et al., 2003). The heat exchangers are designed as TEMA E type shell-and-tube heat exchangers with one shell pass and one tube pass. A 60° triangular tube layout is used; see Figure 2.

Table 3 lists the modelling conditions used for the shell-and-tube heat exchangers including the geometric parameters and the ranges for the flow velocities. The velocities must be high enough to avoid excessive fouling, but not so high that the heat exchanger material is eroded. The boundaries for the flow velocities are selected based on recommendations from Nag (2008), Shah and Sekulić (2003) and Coulson et al. (1999). The shell side velocity is only checked at the inlet, since the density variations of the hot fluid and the cooling water are small. The tube side outlet velocity for the condenser is allowed to be lower than the minimum value of 0.9 m/s for liquid in-tube flow found in Shah and Sekulić (2003). Full liquid flow is only present at the end of the condenser tube as all vapour is condensed. It is, therefore, assumed that the liquid velocity can reach 0.5 m/s at the condenser outlet without the risk of excessive fouling formation.

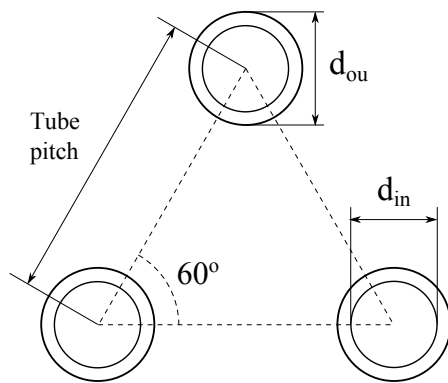


Figure 2: Tube layout

Table 3: Heat exchanger modelling conditions

| Parameter description | Value/range | Unit |
|-----------------------------|-----------------------|------|
| Tube configuration | Rotated square 45° | - |
| Tube thickness | 3 | mm |
| Tube pitch | 1.5 · d _{ou} | mm |
| Baffle cut | 0.25 · d _s | mm |
| Tube wall conductivity | 16 | W/mK |
| Number of control volumes | 30 | - |
| <i>Condenser velocities</i> | | |
| Tube side inlet | 5 – 22 | m/s |
| Tube side outlet | 0.5 – 4 | m/s |
| Shell side inlet | 0.3 – 1.5 | m/s |
| <i>Boiler velocities</i> | | |
| Tube side inlet | 0.9 – 4 | m/s |
| Tube side outlet | 5 – 22 | m/s |
| Shell side inlet | 0.3 – 1.5 | m/s |

The heat transfer and pressure drop characteristics on the shell side are estimated based on the Bell-Delaware method (Shah and Sekulić, 2003). The method is implemented for tubes without fins and for a shell design without tubes in the window section. The effects of larger baffle spacings at the inlet and outlet ducts compared to the central baffle spacing are neglected.

For single-phase flow, the heat transfer coefficient is calculated using the correlation provided by Gnielinski (1976). The two-phase heat transfer coefficient of boiling is estimated based on the correlation provided by Gungor and Winterton (1987) and Thome (1996)

$$\alpha_{2p,boil} = \alpha_L \left[1 + 3000(BoF_c)^{0.86} + 1.12 \left(\frac{x}{1-x} \right)^{0.75} \left(\frac{\rho_L}{\rho_V} \right)^{0.41} \right] \quad (3)$$

where Bo is the boiling number, x is the vapour quality, ρ_L is the density of saturated liquid, ρ_V is the density of saturated vapour and α_L is the liquid only heat transfer coefficient which is calculated using the Dittus-Boelter correlation (Dittus and Boelter, 1930). The ratio of the nucleate boiling heat transfer coefficient to the ideal nucleate boiling heat transfer coefficient, $F_c = \alpha_{nb}/\alpha_{nb,id}$, is calculated by

$$F_c = \left[1 + \left(\frac{\alpha_{nb,id}}{q_{nb}} \right) (T_{dew} - T_{bub}) \left[1 - \exp \left(\frac{-Bq_{nb}}{\rho_L h_{LV} \beta_L} \right) \right] \right]^{-1} \quad (4)$$

where q_{nb} is the nucleate boiling heat flux, T_{dew} is the dew point temperature, T_{bub} is the bubble point temperature, B is a scaling factor, h_{LV} is the enthalpy of vaporization, and β_L is the liquid phase mass transfer coefficient. The values of B and β_L are set to $B = 1$ and $\beta_L = 0.0003$ m/s according to Thome (1996). The ideal nucleate boiling heat transfer coefficient, $\alpha_{nb,id}$ is calculated using the correlation by Stephan and Abdelsalam (1980).

For in-tube condensation, the heat transfer coefficient is estimated using the following correlation (Shah, 2009):

$$\alpha_{2p,cond} = \begin{cases} \alpha_I & J_g \geq 0.98(Z + 0.263)^{-0.62} \\ \alpha_I + \alpha_{Nu} & J_g < 0.98(Z + 0.263)^{-0.62} \end{cases} \quad (5)$$

where Z is Shah's correlating parameter and J_g is the dimensionless vapour velocity.

The heat transfer coefficients α_I and α_{Nu} are calculated as

$$\alpha_I = \alpha_{LT} \left(\frac{\mu_L}{14\mu_V} \right)^{0.0058+0.557P_r} \left[(1-x)^{0.8} + \frac{3.8x^{0.76}(1-x)^{0.04}}{P_r^{0.38}} \right] \quad (6)$$

$$\alpha_{Nu} = 1.32Re_L^{-1/3} \left[\frac{\rho_L(\rho_L - \rho_V)g\lambda_L^3}{\mu_L^2} \right]^{1/3} \quad (7)$$

where α_{LT} is the heat transfer coefficient assuming all mass to be flowing as liquid and Re_L is the Reynolds number for the liquid phase only. The variable α_{LT} is calculated using the Dittus-Boelter equation (Dittus and Boelter, 1930). For mixtures the heat transfer coefficient obtained from equation (5) is corrected using the method proposed by Bell and Ghaly (1973). For in-tube flow, the single-phase pressure drops are calculated based on the Blasius equation (Blasius, 1913) and the two-phase pressure drops are calculated using the correlation by Müller-Steinhagen and Heck (1986).

2.2 Cost Correlations

The cost (in US\$) of the components in the cycle are estimated based on correlations found in the literature. The turbine is assumed to be axial, since axial turbines are commonly used by manufacturers in the range of power (approximately 50-600 kW) considered in the present paper (Quoilin et al., 2013). The cost (in €) of the turbine is estimated based on the correlation provided by Astolfi et al. (2014)

$$C_{turb} = 1.230 \cdot 10^6 \left(\frac{1}{2} \right)^{0.5} \left(\frac{\sqrt{\dot{V}_4}/(\Delta h_{is})^{0.25}}{0.18} \right)^{1.1} \quad (8)$$

where \dot{V}_4 is the volume flow at the turbine outlet and Δh_{is} is the isentropic enthalpy drop across the turbine. An euro-to-dollar conversion factor of 1.2 is used to convert the turbine cost to US\$.

The costs of the pumps, the heat exchangers and the generator are estimated by

$$C_E = C_B \left(\frac{Q}{Q_B} \right)^M f_M f_P f_T \quad (9)$$

where C_E is the equipment cost for equipment with capacity Q , C_B is the base cost for equipment with capacity Q_B , M is a constant exponent, and f_M , f_P are f_T correction factors accounting for materials of construction, design pressure and design temperature.

The economic parameters needed in the cost correlation are listed in Table 4. For the heat exchangers, the pressure correction factor is obtained by linear interpolation between the values reported in Smith (2005). The component costs are corrected for inflation by using the Chemical Engineering Plant Cost Index.

Table 4: Economic parameters

| Component | C_B | Q_B | M | f_M | f_P | f_T | Reference |
|-----------------|----------|-------------------|------|-------|---------------|-------|---------------|
| Heat exchangers | 32.8 k\$ | 80 m ² | 0.68 | 1.7 | (Smith, 2005) | 1 | (Smith, 2005) |
| Pumps | 9.48 k\$ | 4 kW | 0.55 | 1 | | 1 | (Smith, 2005) |
| Generator | 3.7 k\$ | 1000 kW | 0.95 | 1 | | 1 | (Boehm, 1987) |

3. RESULTS AND DISCUSSION

Figure 3 shows the Pareto fronts for multi-objective optimizations of net power output and cost for R32, R134a and R32/R134a (0.65/0.35). The results indicate that R32/R134a is the best of the three fluids, since it enables the highest net power output at the lowest component cost. R32 is the second best fluid while R134a is performing worst.

When the fluids are compared based on a single-objective optimization of net power output, R32/R134a (0.65/0.35) reaches 13.8 % higher net power output than R32 and 14.6 % higher than R134a (Andreasen et al., 2014). However, this approach does not account for the equipment cost, and it was therefore not ensured that the fluids were compared based on similar cost. The multi-objective optimization, on the other hand, does enable a fluid comparison based on fixed equipment cost. For a total cost of 1200 k\$, R32/R134a reaches a 3.4 % higher net power than R32 and 10.9 % higher than R134a. At $C_{tot} = 800$ k\$, the mixture obtains 2.1 % higher net power than R32 and 12.6 % higher than R134a. It should be noted that in the single-objective optimization, which was presented in Andreasen et al. (2014), the mixture composition was optimized, but in the multi-objective optimization, carried out in the present paper, it is not. It is, therefore, possible that higher performance can be achieved with the mixture if the composition is optimized in the multi-objective optimization.

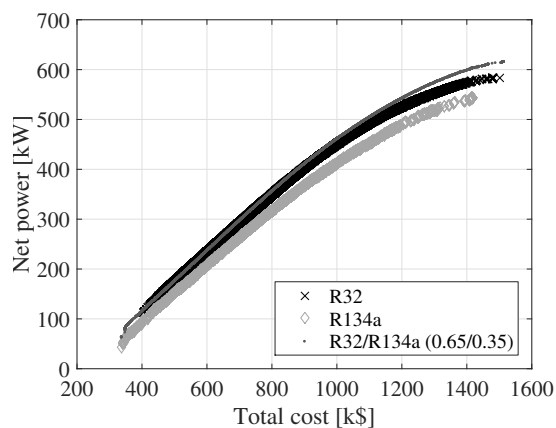


Figure 3: Pareto fronts

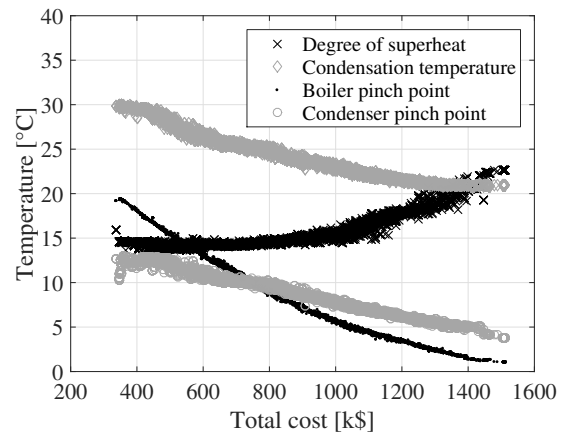


Figure 4: Temperatures, R32/R134a

In Figure 4, the optimal degree of superheating, condensing temperature, boiler pinch point and condenser pinch point are plotted as a function of the total cost for R32/R134a. The degree of superheating increases from about 13 to 23 °C as the total component cost increases. The condensing temperature, boiler pinch point and condenser pinch point all continuously decrease as the total component cost increases. The decrease in boiler pinch point results in an increase in the heat input to the cycle. This trend positively affects the net power output while increasing the investment cost for the boiler. The decrease in the condensing temperature has a positive effect on net power output, but requires larger heat

transfer areas since the temperature difference between the cooling water and the condensing working fluid decreases. The larger heat transfer areas result in higher investment costs for the condenser. For fixed cycle conditions (condensing temperature, mass flow, etc.), the condenser pinch point only affects the net power output of the cycle through the power consumption of the cooling water pump. The pinch point temperature of the condenser thereby primarily affects the cost of the condenser. Therefore, the condenser pinch point tends to be as large as possible, while respecting the following constraints: 1) the cooling water outlet temperature must be larger than the inlet temperature and 2) the flow velocity in the condenser shell should not be higher than 1.5 m/s. A high condenser pinch point results in a low cooling water temperature increase and thereby a high cooling water mass flow and a high shell flow velocity. For R32/R134a, the temperature glide of condensation is 5.3 °C, while the cooling water temperature increase ranges from 5.7 to 14.5 °C. In thermodynamic analyses of zeotropic mixtures, optimum conditions are typically obtained when the temperature glide of the mixture and the temperature increase of the cooling water are matched (Heberle et al., 2012; Chys et al., 2012; Lecompte et al., 2014; Andreasen et al., 2014). The present study does on the other hand indicate that optimum conditions are reached when the temperature increase of the cooling water is larger than the temperature glide of condensation.

For total costs of 1300 k\$, the boiler pinch point drops below 2.5 °C. It is unusual that solutions with pinch points below 2.5 °C represent economically feasible solutions. In Figure 3 at a total cost of 1300 k\$, the curves are levelling off, meaning that an increase in investment cost results in a low increase in net power output compared to when the total cost is lower. It is therefore likely that the more economically feasible solutions are found at total costs below 1300 k\$. It should be noted that the Pareto fronts do not provide information which directly can be used to make an investment decision, since they do not include information about the possible income related to the power delivered by the ORC power plant. Such information is necessary in order to estimate, e.g., net present value or payback periods which are useful figures for making investment decisions. The Pareto fronts should rather be used for assessing the feasibility of working fluids based on equal component costs, thereby ensuring a fair basis for comparison.

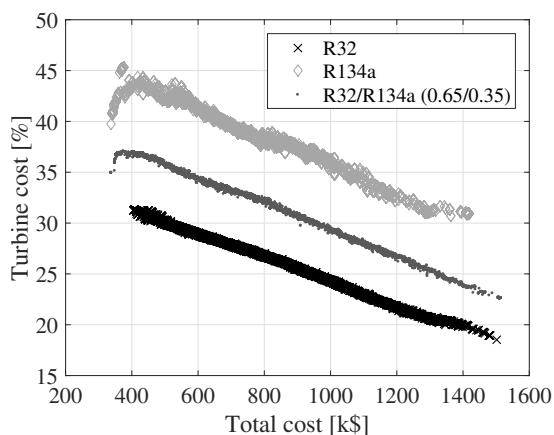


Figure 5: Relative turbine costs

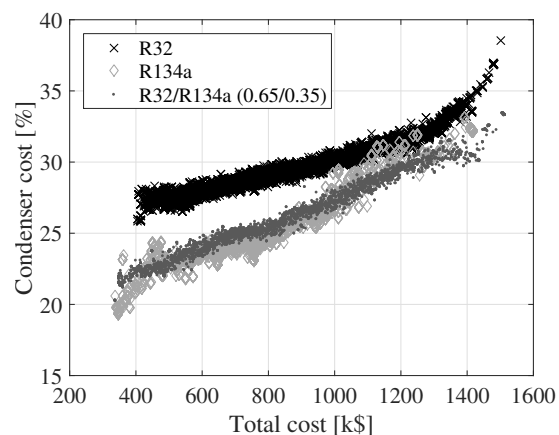


Figure 6: Relative condenser costs

Figures 5, 6 and 7 depict the variation of the cost of the turbine, condenser and boiler as a function of the total cost for the three fluids. The cost values displayed on the y-axes are relative to the total cost. The relative size of the turbine cost decreases, while the relative costs of the condenser and boiler increase. The relative turbine costs decreases since the turbine cost is a function of the turbine outlet volume flow rate and the isentropic enthalpy drop across the turbine. An increase in the outlet volume flow rate or a decrease in the isentropic enthalpy drop results in an increase in the turbine cost. These two parameters can be varied by changing e.g. the boiler pressure or the turbine inlet temperature. By modifying the boiler pressure or the turbine inlet temperature it is, however, not certain that the net power output increases. The cost of the condenser and the boiler can be increased by decreasing the

pinch point temperatures of the heat exchangers or the condensing temperature. This has a positive effect on the net power output. Thus, the cost of the heat exchangers are not as tightly connected to the cycle as the turbine is.

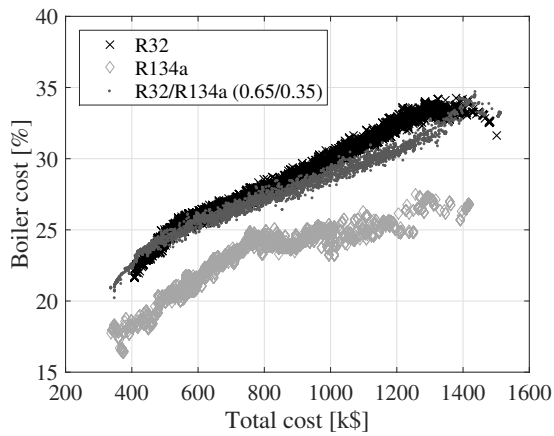


Figure 7: Relative boiler costs

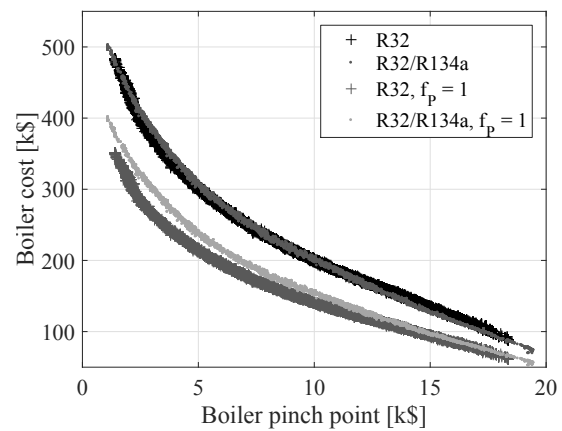


Figure 8: Boiler cost comparison

The boiler pressures range from 39-45 bar for R32, 28-35 bar for R32/R134a and 16-22 bar for R134a. Correspondingly the critical pressures are 57.8 bar, 51.8 bar and 40.6 bar for R32, R32/R134a and R134a, respectively, thus indicating that higher critical pressures are related to higher optimum boiling pressures. Figure 8 displays a comparison of the boiler costs for R32 and R32/R134a with and without the pressure correction factor (f_p). The boiler pinch point is plotted on the x-axis. It is, thereby, possible to compare the boiler costs for a given pinch point temperature difference. When the pressure correction factor is unity, the boiler costs are higher for the mixture compared to R32. When the pressure correction factor is employed as a function of the boiler pressure, the boiler costs are similar for the two fluids. This indicates that the boiler pressure reduction, achieved when using the mixture, can compensate for the increase in boiler cost caused by the degradation of the heat transfer coefficient and the lower temperature difference of heat transfer.

For R32/R134a, the shell length to diameter ratio of the shell-and-tube heat exchanger designs are in a range of 37-110 for the condenser and 76-180 for the boiler. Shah and Sekulić (2003) advise a desirable range of 3-15 for this ratio, meaning that the condensers and the boilers should consist of numerous shorter shell-and-tube heat exchangers in series, in order not to violate this practical limit. The shells designed in this paper are long since the number of tubes must be relatively low in order to ensure reasonable flow velocities in the tubes. Selecting a heat exchanger layout with multiple tube passes is a viable solution for increasing the number of tubes while maintaining high flow velocities in the tubes. Another option is to place the working fluid in the shell rather than in the tubes. This would increase the risk of working fluid leakage, which is problematic in the case of zeotropic mixtures.

4. CONCLUSION

This paper presents the results from a multi-objective optimization of net power output and component cost for ORC power plants using R32, R134a and R32/R134a (0.65/0.35_{mole}). For a low-temperature heat source, the results indicate that R32/R134a (0.65/0.35) is the best fluid and that R134a performs worst. For a total cost of 1200 k\$, the mixture reaches 3.4 % higher net power than R32 and 10.9 % higher than R134a. The relative increase in net power output for the mixture compared to R32 is significantly lower than the 13.8 %, which was estimated in a single-objective optimization of net power, i.e., not considering the cost of the cycle components. This exemplifies the importance of accounting for economic criteria in ORC system optimizations and fluid comparisons. This is especially important when pure fluids and mixtures are compared due to the generally lower temperature difference of heat transfer

and the degradation of heat transfer coefficients for zeotropic mixtures. Moreover, the differences in operating pressures can have a significant effect on the cost of the ORC power plant. It is thus possible to reduce the cost of the boiler by using R32/R134a as the working fluid compared to R32, since the optimum pressure is lower for the mixture.

Future work on this topic will include performance comparisons for a larger group of pure fluids and mixtures and an extension of the economic analysis enabling the estimation of payback periods and net present values, such that the more cost efficient working fluids can be identified. An uncertainty analysis, assessing the influence of the uncertainties related to heat transfer and equipment cost correlations, is also a topic for further investigation, especially in the light of the relatively small performance differences observed for R32 and R32/R134a.

NOMENCLATURE

| Symbol | | | Subscript | |
|----------------|-------------------------------|--------------------------|-----------|--------------------|
| A | heat transfer area | (m ²) | 1p | one-phase |
| B | scaling factor | () | 2p | two-phase |
| Bo | boiling number | () | B | base |
| C | cost | (US\$) | boil | boiler |
| d | diameter | (mm) | bub | bubble point |
| f | correction factor | () | c | critical |
| F _c | $\alpha_{nb}/\alpha_{nb,id}$ | () | cond | condenser |
| g | gravitational acceleration | (m/s ²) | cool | cooling water |
| G | mass flux | (kg/(s m ²)) | dew | dew point |
| h | specific enthalpy | (kJ/kg) | E | equipment |
| J _g | dimensionless vapour velocity | () | gen | generator |
| M | Exponent in cost correlation | () | HEX | heat exchanger |
| m | mass flow rate | (kg/s) | i | inlet |
| P | pressure | (bar) | id | ideal |
| Q | equipment capacity | (m ²), (kW) | in | inner |
| q | heat flux | (kW/m ²) | is | isentropic |
| Re | Reynolds number | () | L | saturated liquid |
| T | temperature | (°C) | LT | all mass as liquid |
| \dot{V} | volume flow | (m ³ /s) | LV | vaporization |
| \dot{W} | work | (kW) | nb | nucleate boiling |
| x | vapour quality | () | NET | net |
| Z | Shah's correlating parameter | () | ou | outer |
| α | heat transfer coefficient | (W/(m ² K)) | pump | pump |
| β | mass transfer coefficient | (m/s) | r | reduced |
| Δ | difference | () | s | shell |
| λ | thermal conductivity | (W/(m K)) | tot | total |
| μ | viscosity | (kg/(s m)) | turb | turbine |
| ρ | density | (kg/m ³) | V | saturated vapour |
| | | | wf | working fluid |

REFERENCES

Andreasen, J. G., Larsen, U., Knudsen, T., Pierobon, L., and Haglind, F. (2014). Selection and optimization of pure and mixed working fluids for low grade heat utilization using organic Rankine cycles. *Energy*, 73:204–213.

- Angelino, G. and Colonna, P. (1998). Multicomponent working fluids for organic Rankine cycles (ORCs). *Energy*, 23(6):449–463.
- Astolfi, M., Romano, M. C., Bombarda, P., and Macchi, E. (2014). Binary ORC (Organic Rankine Cycles) power plants for the exploitation of medium-low temperature geothermal sources - Part B: Techno-economic optimization. *Energy*, 66:435–446.
- Bell, K. and Ghaly, M. (1973). An approximate generalized design method for multicomponent/partial condenser. *AIChE Symp. Ser.*, 69:72–79.
- Blasius, H. (1913). Das Ähnlichkeitsgesetz bei Reibungsvorgängen in Flüssigkeiten. In *Mitteilungen über Forschungsarbeiten auf dem Gebiete des Ingenieurwesens 131*, pages 1–41. Springer, Berlin, Germany.
- Boehm, R. F. (1987). *Design analysis of thermal systems*. John Wiley & Sons, Inc., New York, United States of America.
- Cavallini, A., Censi, G., Del Col, D., Doretti, L., Longo, G., Rossetto, L., and Zilio, C. (2003). Condensation inside and outside smooth and enhanced tubes — a review of recent research. *Int. J. Refrig.*, 26(4):373–392.
- Chys, M., van den Broek, M., Vanslambrouck, B., and De Paepe, M. (2012). Potential of zeotropic mixtures as working fluids in organic Rankine cycles. *Energy*, 44(1):623–632.
- Coulson, J., Richardson, J., and Backhurst, J. (1999). *Coulson and Richardson's Chemical Engineering*. Butterworth-Heinemann, Oxford, Great Britain.
- Dittus, W. and Boelter, L. M. K. (1930). Heat transfer in automobile radiators of the tubular type. *Univ. Calif. – Publ. Eng.*, 2(13):443 – 461.
- Gnielinski, V. (1976). New Equation for Heat and Mass Transfer in Turbulent Pipe and Channel Flow. *Int. Chem. Eng.*, 16:359–368.
- Gungor, K. E. and Winterton, R. H. S. (1987). Simplified general correlation for saturated flow boiling and comparisons of correlations with data. *Chem. Eng. Res. Des.*, 65(2):148–156.
- Heberle, F., Preißinger, M., and Brüggemann, D. (2012). Zeotropic mixtures as working fluids in Organic Rankine Cycles for low-enthalpy geothermal resources. *Renew. Energy*, 37(1):364–370.
- Kærn, M. R., Modi, A., Jensen, J. K., and Haglind, F. (2015). An Assessment of Transport Property Estimation Methods for Ammonia–Water Mixtures and Their Influence on Heat Exchanger Size. *Int. J. Thermophys.*
- Le, V. L., Kheiri, A., Feidt, M., and Pelloux-Prayer, S. (2014). Thermodynamic and economic optimizations of a waste heat to power plant driven by a subcritical ORC (Organic Rankine Cycle) using pure or zeotropic working fluid. *Energy*, 78:622–638.
- Lecompte, S., Ameel, B., Ziviani, D., van den Broek, M., and De Paepe, M. (2014). Exergy analysis of zeotropic mixtures as working fluids in Organic Rankine Cycles. *Energy Convers. Manag.*, 85:727–739.
- Lemmon, E. W., Huber, M., and McLinden, M. (2013). NIST Standard Reference Database 23: Reference Fluid Thermodynamic and Transport Properties-REFPROP, Version 9.1, National Institute of Standards and Technology, Standard Reference Data Program, Gaithersburg.
- Mathworks (2014). Matlab 2014b documentation. Technical report, Massachusetts, The United States of America.

- Müller-Steinhagen, H. and Heck, K. (1986). A simple friction pressure drop correlation for two-phase flow in pipes. *Chem. Eng. Process. Process Intensif.*, 20(6):297–308.
- Nag, P. K. (2008). *Power Plant Engineering*. Tata McGraw Hill Education Private Limited, New Delhi, India, 3 edition.
- Pierobon, L., Benato, A., Scolari, E., Haglind, F., and Stoppato, A. (2014). Waste heat recovery technologies for offshore platforms. *Appl. Energy*, 136:228–241.
- Quoilin, S., van den Broek, M., Declaye, S., Dewallef, P., and Lemort, V. (2013). Techno-economic survey of Organic Rankine Cycle (ORC) systems. *Renew. Sustain. Energy Rev.*, 22:168–186.
- Shah, M. M. (2009). An Improved and Extended General Correlation for Heat Transfer During Condensation in Plain Tubes. *HVAC&R Res.*, 15(5):889–913.
- Shah, R. K. and Sekulić, D. P. (2003). *Fundamentals of Heat Exchanger Design*. John Wiley & Sons, Inc., New Jersey, United States of America.
- Smith, R. (2005). *Chemical process: design and integration*. John Wiley & Sons, Inc., West Sussex, England.
- Stephan, K. and Abdelsalam, M. (1980). Heat-transfer correlations for natural convection boiling. *Int. J. Heat Mass Transf.*, 23(1):73–87.
- Thome, J. R. (1996). Boiling of new refrigerants: a state-of-the-art review. *Int. J. Refrig.*, 19(7):435–457.
- Trapp, C. and Colonna, P. (2013). Efficiency Improvement in Precombustion CO₂ Removal Units With a Waste-Heat Recovery ORC Power Plant. *J. Eng. Gas Turbines Power*, 135(4):042311.

ACKNOWLEDGEMENT

The work presented in this paper has been conducted within the frame of the THERMCYC project ("Advanced thermodynamic cycles utilising low-temperature heat sources"; see <http://www.thermcyk.mek.dtu.dk/>) funded by InnovationsFonden, The Danish Council for Strategic Research in Sustainable Energy and Environment. The financial support is gratefully acknowledged.